SEISMIC BEHAVIOR OF COUPLING BEAMS CONSTRUCTED WITH VARIOUS TYPES OF STEEL FIBER REINFORCED CONCRETE

A. Pérez-Irizarry[1], G.J. Parra-Montesinos[2]

[1] *Graduate Student Research Assistant, University of Wisconsin-Madison, perezirizarr@wisc.edu*
[2] *C.K. Wang Professor of Structural Engineering, University of Wisconsin-Madison, gustavo.parra@wisc.edu*

Abstract

An experimental study was conducted to evaluate the use of various types of steel fiber reinforced concrete (SFRC) in order to eliminate the need for diagonal bars and relax transverse reinforcement requirements in earthquake-resistant coupling beams. Eight precast, large-scale coupling beam specimens, five with a span-to-depth ratio (l_n/h) of 3.0 and three with l_n/h = 2.0, were tested under large displacement reversals. In addition to the span-to-depth ratio, experimental variables were: 1) type of SFRC (fiber type and dosage); and 2) peak shear stress demand. Three types of hooked steel fibers were evaluated in volume fractions of 1.0%, 1.25% or 1.5% for a total of six SFRC mixtures investigated. Peak shear stress demand, on the other hand, ranged between approximately 6 and $12\sqrt{f_c'}$ [psi]. In addition to the coupling beam tests, all SFRC materials investigated were tested under four-point bending, direct tension and compression in order to correlate material behavior with coupling beam seismic performance.

In general, SFRC coupling beams without diagonal reinforcement and with $l_n/h \geq 2.0$ can achieve drift capacities of at least 5% when subjected to shear stress reversals of magnitude ranging from 6 to $10\sqrt{f_c'}$ [psi]. The behavior of all the SFRC coupling beams was heavily controlled by flexural deformations, which contributed approximately 70-80% to the total applied drift. For design purposes and based on test results, three classes of SFRCs are proposed depending on their performance under four-point bending. Limits to coupling beam shear stress and span-to-depth ratio are linked to each of the three classes of SFRC in order to achieve a drift capacity of at least 6%.

The transverse reinforcement requirements for potential plastic hinge regions in columns of special moment frames in ACI 318-14 were found to be adequate to provide confinement to the end regions of coupling beams, over half the beam depth from the wall faces. Transverse reinforcement in the middle region of SFRC coupling beams, on the other hand, must be designed such that the expected shear stress resisted by the SFRC does not exceed a limit of 4, 3 and $2\sqrt{f'_c}$ [psi] for coupling beams constructed with SFRC Class 1, 2 and 3, respectively.

Expected flexural capacity can be estimated based on the use of a plastic stress distribution assuming all reinforcement over the tension half of the beam depth reaches a stress of 1.1 times the measured yield strength or 1.25 times the nominal yield strength. It is also recommended that strength calculations be ran without axial force and with an axial force of $0.1f'_cA_g$. For adequate spread of plasticity, intermediate dowel reinforcement at the beam ends must be designed such that the shear associated with the expected flexural strength at the end of the dowels, neglecting the SFRC post-cracking strength, ranges between 1.0 and 1.1 times the shear corresponding to the expected flexural strength at the beam end.

Keywords: drift capacity; shear strength; coupled walls; steel fibers.

1. Introduction

The behavior of coupled structural walls during strong earthquakes is greatly influenced by the strength, stiffness and energy dissipation capacity of coupling beams. Given their low span-to-depth ratio (typically less than 3.5) and expected high shear stress demand (often greater than $6\sqrt{f_c'}$ [psi], where f_c' is the concrete compressive strength), the design and construction of these coupling beams have long represented a challenge to structural engineers and contractors.

Current design practice for coupling beams in regions of high seismicity is primarily based on results from research conducted in the late 1960s and early 1970s in New Zealand (Paulay 1971; Paulay and Binney, 1974; Paulay and Santhakumar, 1976). The design generally incudes the use of diagonal bars in sufficient amounts such as to resist the entire design shear force. Further, transverse reinforcement similar to that used in potential plastic hinge regions of columns of special moment resisting frames is required to provide confinement to either the diagonal reinforcing bars or the entire coupling beam. As shown in Fig. 1, this design is difficult to construct given the intricate reinforcement detailing involved and the need to "thread" diagonal bars through heavily congested wall boundary regions.

Fig. 1 – Reinforcement congestion in a diagonally reinforced coupling beam (courtesy of Rémy Lequesne)

As an alternative to the reinforcement detailing discussed above, the use of fiber reinforcement has been extensively investigated in order to evaluate its potential to substantially simplify the design of coupling beams (Canbolat, Parra-Montesinos and Wight, 2005; Lequesne, 2011; Setkit, 2012; Lequesne, Parra-Montesinos and Wight, 2013; Parra-Montesinos et al., 2014). As part of this effort, one design has been recommended for use in relatively slender coupling beams (span-to-depth ratios greater than or equal to 2.2). This design consists of the use of longitudinal and transverse reinforcement only (i.e., no diagonal bars), with column-type special confinement at the beam ends over a length half the beam depth from the wall faces. This reinforcement design, when used in combination with 1.2 in. long and 0.015 in. diameter hooked steel fibers with a nominal tensile strength of 330 ksi, has been shown to lead to drift capacities of at least 5% in coupling beams subjected to shear stress levels comparable to the maximum limit allowed in ACI 318-14 (ACI Committee 318, 2014) for diagonally reinforced coupling beams ($10\sqrt{f_c'}$ [psi]). The significant simplifications in reinforcement detailing achieved through the use of this fiber reinforced concrete has led to the recent implementation of this design in two high-rise building projects in the State of Washington, USA (Parra-Montesinos et al., 2014; Kopczynski and Whiteley, 2016).

The wide implementation of a fiber reinforced concrete coupling beam design in the United States and elsewhere requires, among other things, the specification of performance criteria for fiber reinforced concrete such that the design is not tied to the use of a particular type of fiber at a given amount. Ideally, structural designers should be able to specify material performance criteria that would "ensure" a minimum coupling beam seismic performance (e.g., minimum drift capacity for a given expected shear stress). Towards this end, an

experimental research program was conducted in order to evaluate the seismic performance of coupling beams constructed with various types of steel fibers and in different dosages. A description of and results from this experimental program are presented herein.

2. Experimental program

Eight coupling beam specimens were tested under lateral displacement reversals. Each coupling beam specimen consisted of a precast, rectangular coupling beam connected to two large rectangular blocks that simulated the end regions of two walls being coupled. Main variables investigated were: 1) coupling beam span-to-depth ratio, l_n/h (3.0 and 2.0); 2) peak shear stress demand ($6 - 12\sqrt{f'_c}$ [psi]); and 3) type of fiber reinforced concrete (i.e., fiber type and dosage).

   Reinforcement detailing for all coupling beam specimens is shown in Fig. 2. As can be seen, typical reinforcement layout consisted of main top and bottom longitudinal reinforcement, intermediate longitudinal bars, closely spaced double-hoop confinement reinforcement at the beam ends, and single hoops in the middle region of the beam. U-shaped dowels were also used to strengthen the cold joint between the precast coupling beam and the end blocks, preventing concentration of inelastic deformations at this joint and the development of a premature sliding shear failure.
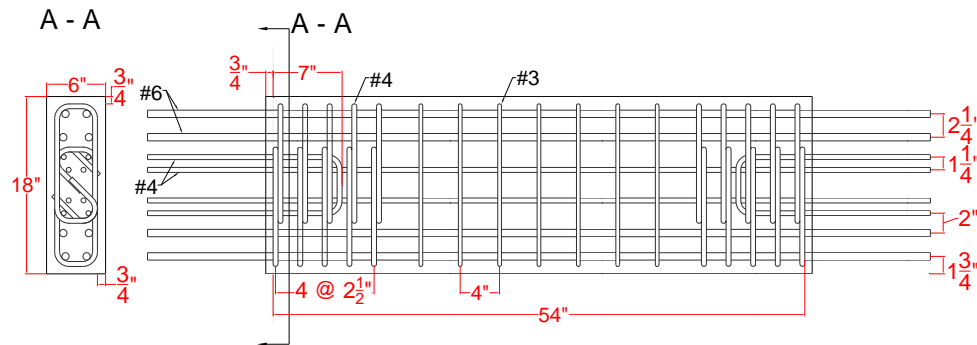
a)   Coupling Beam CB1
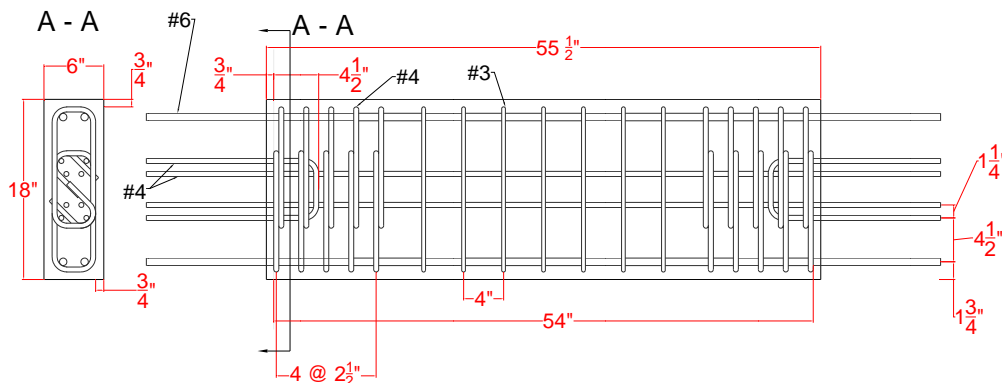
b)   Coupling Beams CB2 and CB3
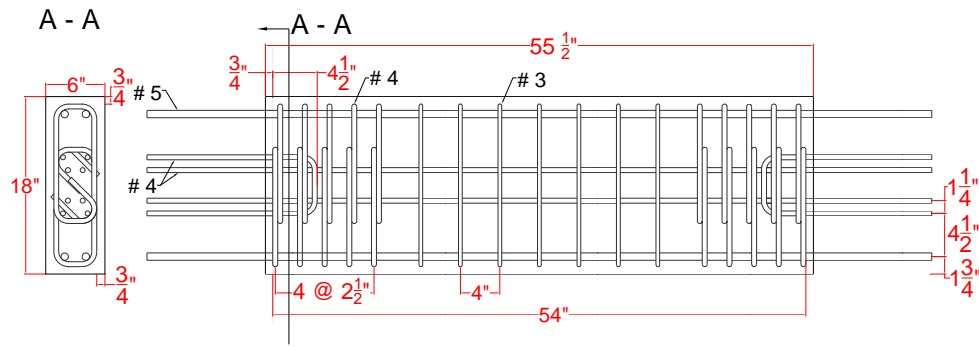
c) **Coupling Beams CB4 and CB5**
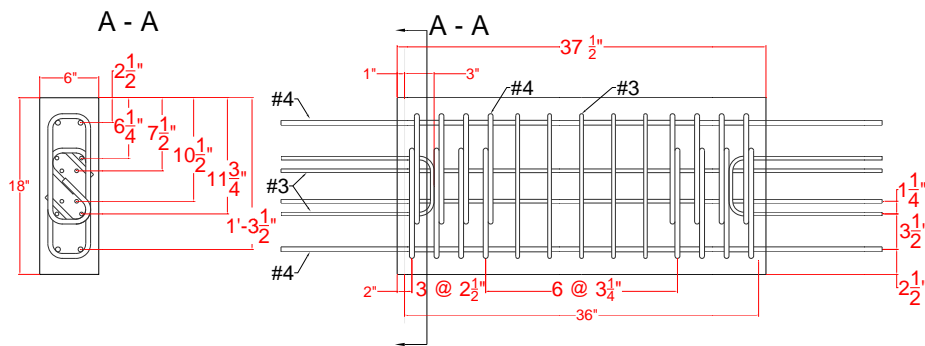
d) **Coupling Beam CB6**
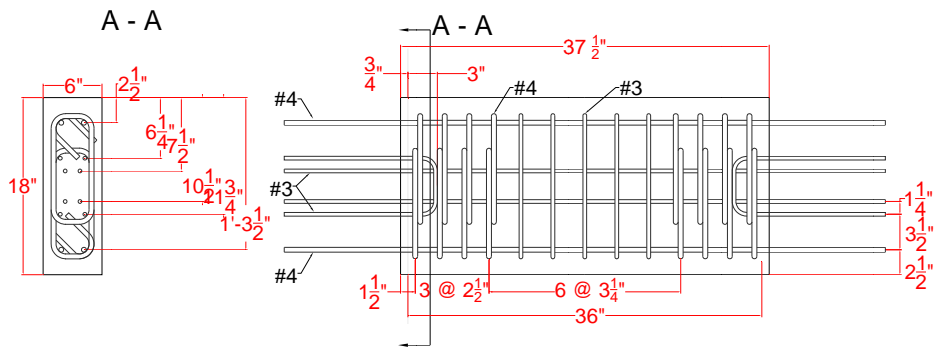
e) **Coupling Beams CB7 and CB8**

Fig. 2 – Reinforcement detailing of coupling beam specimens

The SFRCs considered in this experimental work had, on average, a compressive strength of approximately 9000 psi. Three different hooked steel fibers were evaluated, HE 55/35, RC 55/30 BG and RC 80/30 BP fibers, with a nominal tensile strength of 195 ksi, 174 ksi and 330 ksi, respectively. HE 55/35 fibers were manufactured by ArcelorMittal and both RC 55/30 BG and RC 80/30 BP fibers were manufactured by Bekaert Corporation. Figure 3 shows the geometry of the three fibers investigated.

A total of six different SFRCs were investigated. The selection of a particular SFRC depended on the beam span-to-depth ratio and shear stress demand. In general, coupling beams constructed with the SFRCs expected to show the best performance were designed for higher shear stress demands (approximately $8 -$

$12\sqrt{f'_c}$ [psi]). Coupling beams constructed with lower performing SFRCs, on the other hand, were designed for shear stresses approximately $6 - 8\sqrt{f'_c}$ [psi]. Also, materials expected to perform the best were used in the coupling beams with $l_n/h = 2.0$ given the increased role played by shear in these beams compared to those with $l_n/h = 3.0$. All SFRC materials evaluated had the same concrete proportions by weight as follows, 1.2:0.30:1.7:1.0:0.5 for Portland Cement Type 1:Class C Fly Ash:Torpedo sand:coarse aggregate (3/8 in. maximum size):water. A summary of some of the main features of the test specimens is provided in Table 1.
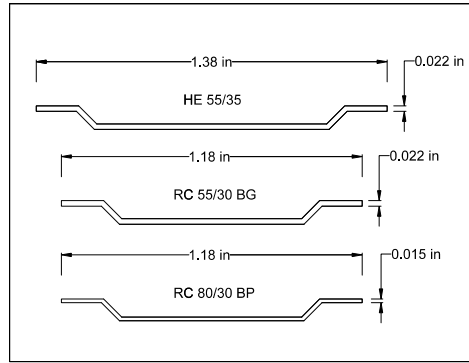
Fig. 3 – Geometry of steel fibers evaluated

Table 1 - Summary of coupling beam main features and key response parameters

Specimen	f'_c (psi)	Fiber type	V_f (%)	V_u (kips)	v_u (psi)	$v_u/\sqrt{f'_c}$	P_u (kips)	Drift	
								20% loss	30% loss
CB1	7930	HE55/35	1.25	117	1080	12.2	89	3.4%	3.4%
CB2	8840	HE55/35	1.25	100	930	9.8	144	5.5%	6.5%
CB3	8630	RC55/30BG	1.25	95	880	9.5	116	6.7%	6.7%
CB4	9260	RC55/30BG	1.0	75	690	7.2	99	5.2%	6.2%
CB5	9750	RC80/30BP	1.0	83	770	7.8/6.6**	91	6.2%*	6.7%*
CB6	7950	H55/35	1.5	78	720	8.1/7.3**	74	5.1%*	6.1%*
CB7	9330	RC80/30BP	1.5	105	970	10.1	125	5.3%	5.3%
CB8	8490	RC80/30BP	1.5	82	760	8.2	90	6.2%	7.7%

* Reported drifts based on peak strength reached after adjustment of axial force
** Peak shear stress after adjustment of axial force
V_f: fiber volume fraction; V_u: peak shear force; v_u: peak average shear stress based on gross area; P_u: peak axial load

For testing convenience, each coupling beam specimen was rotated 90 degrees. Figure 4 shows the test setup used. Due to laboratory limitations, each specimen was loaded through a "rigid" steel arm connected to the top block at one end and to a hydraulic actuator at the other end. Two vertical steel links were used to keep the top block horizontal while providing some degree of axial growth restraint to the coupling beam. All specimens except CB1 were subjected to displacement reversals starting at 0.25% (drift is equal to chord rotation of the coupling beam) up to failure, with increments of 0.25% for cycles of up to 1.0% drift, of 0.5% for cycles between 1.0% and 2.0% drift, and of 1.0% for larger displacement cycles.
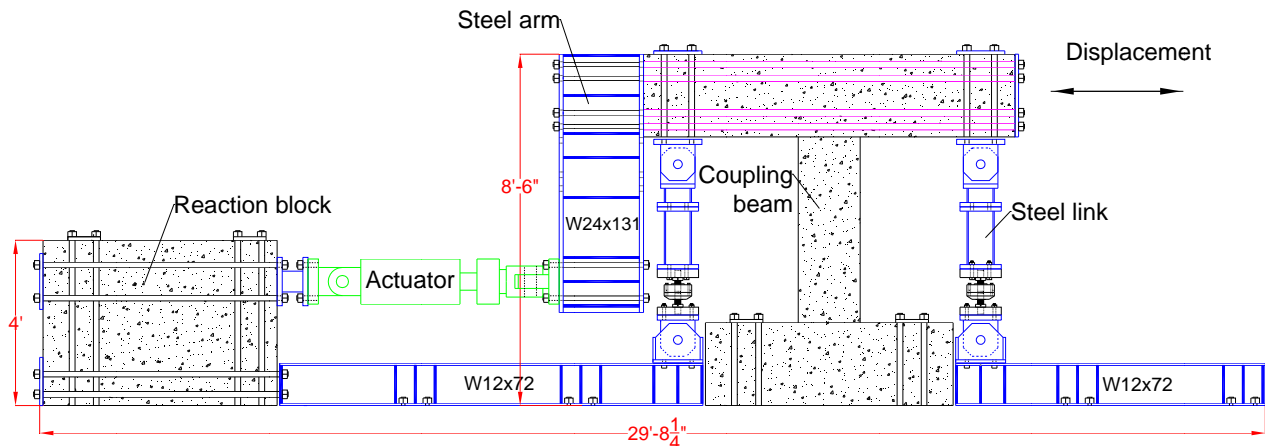
Fig. 4 – Test setup

3. Experimental results

3.1 Flexural and tensile behavior of SFRCs

The behavior of the various SFRCs investigated was evaluated through bending, direct tension and compression tests. In this paper, only the results from four-point bending tests of un-notched beams and direct tensile tests of notched prisms are presented.

The specimens subjected to four-point bending were 6 in. x 6 in. in cross section with a span length of 18 in. The specimens subjected to direct tension, on the other hand, had a 6 in. square cross section with a length of 14 in. A 3/4 in. notch was saw cut around the specimen perimeter at the mid-length section for evaluation of average tensile stress versus crack width behavior. Tension was introduced to the SFRC prism through a steel reinforcing bar embedded into each end of the concrete prism.

The average results from the four-point bending tests of un-notched beams and direct tensile tests of notched prisms are shown in Figs. 5a and 5b, respectively. The flexural response is shown in terms of equivalent bending stress f_{eq}, calculated assuming linear elastic behavior with uncracked section properties, normalized by the first cracking strength f_{cr}. The tensile response is expressed in terms of average tensile stress f_t, normalized by $\sqrt{f'_c}$ [psi]. As can be seen, the SFRC materials with a 1.5% volume fraction exhibited deflection hardening response. All other materials exhibited a peak post-cracking flexural strength ranging between 0.75 and 0.95 of the first cracking strength. Under direct tension, only the SFRC material with RC 80/30 BP fibers at a 1.5% volume fraction exhibited a post-cracking strength greater than the first cracking strength. All other SFRC materials exhibited substantially lower post-cracking tensile strengths.

3.2 Coupling Beam Overall behavior

All test coupling beam specimens, except Coupling Beam CB1, exhibited a stable behavior under large displacement reversals with peak average shear stresses ranging between approximately 7 and $10\sqrt{f'_c}$ [psi]. Coupling beam drift capacity in these specimens was at least 5%, with flexural deformations accounting for approximately 70% to 80% of the applied drift. Drift capacity was defined as the average of the peak positive and negative drift of the last cycle completed prior to a strength loss greater than 20% of the peak strength in either loading direction. In Coupling Beam CB1, the amount of longitudinal reinforcement was greater than that in all other specimens, which translated into a higher peak shear stress in the coupling beam ($12.2\sqrt{f'_c}$ [psi]) and an estimated peak shear stress demand on the SFRC greater than $6\sqrt{f'_c}$ [psi]. Such high shear stresses led to a premature shear failure with a drift capacity slightly greater than 3% drift.

6

a) Four-point bending tests

b) Direct tensile tests

c)
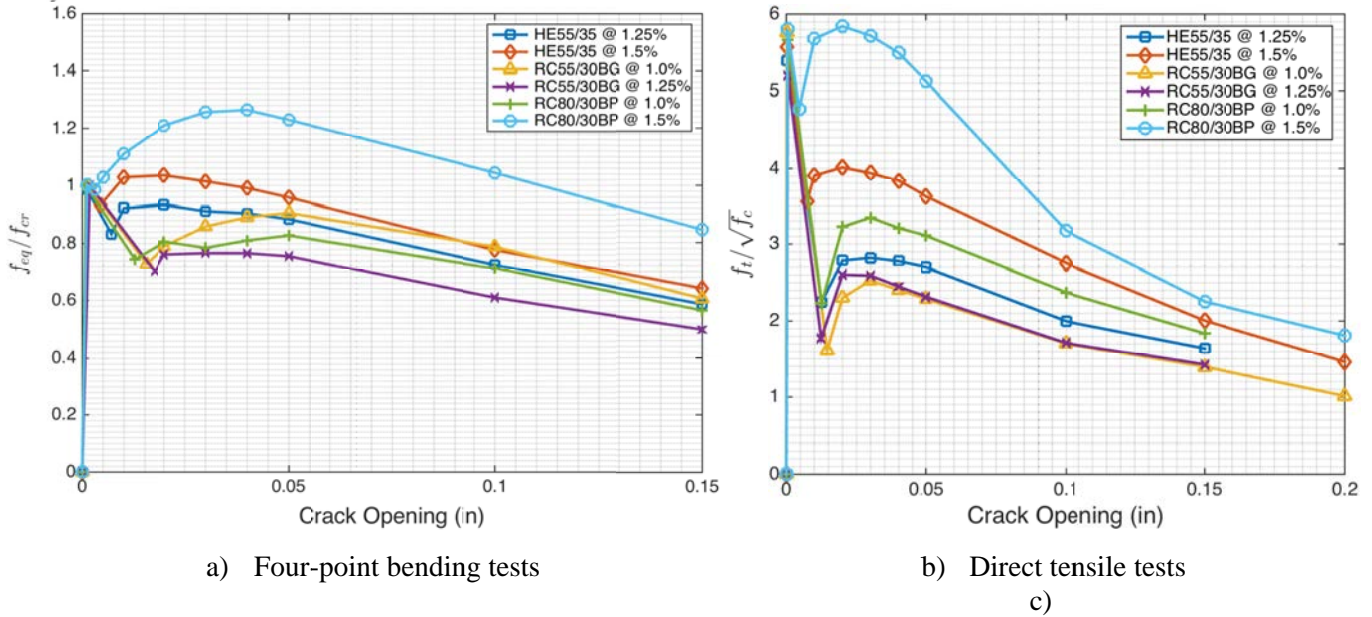
Fig. 5 – Flexural and tensile response of SFRCs

In general, early cracking in the coupling beams consisted of flexural cracks at the beam ends and diagonal cracks in the middle region of the beam. Except for Coupling Beam CB1, diagonal cracks in the middle region of the beam remained narrow, while flexural cracks at the beam ends widened as lateral displacements increased and reinforcement yielding developed at the beam ends. At large drifts, typically 4% and greater, significant damage could be observed at the beam ends, characterized by some concrete crushing and spalling, and the joining of flexural cracks corresponding to both loading directions, which typically led to a through-depth crack at each beam ends. Ultimately, significant shear sliding developed along these through cracks, leading to a substantial loss of lateral stiffness and energy dissipation capacity.

Axial elongation of the coupling beams during displacement cycles, caused by concrete cracking and reinforcement yielding, led to the development of meaningful axial forces in the coupling beams during the tests. In all specimens except Coupling Beam CB2, the peak average axial stress developed ranged between $0.09f'_c$ and $0.12f'_c$, calculated based on the gross cross-section area. The peak axial stress in Specimen CB2, on the other hand, was $0.15f'_c$. Average peak axial strain in Specimens CB2 through CB8 ranged between 0.5% and 0.9%.

a) Specimen CB2

b) Specimen CB5
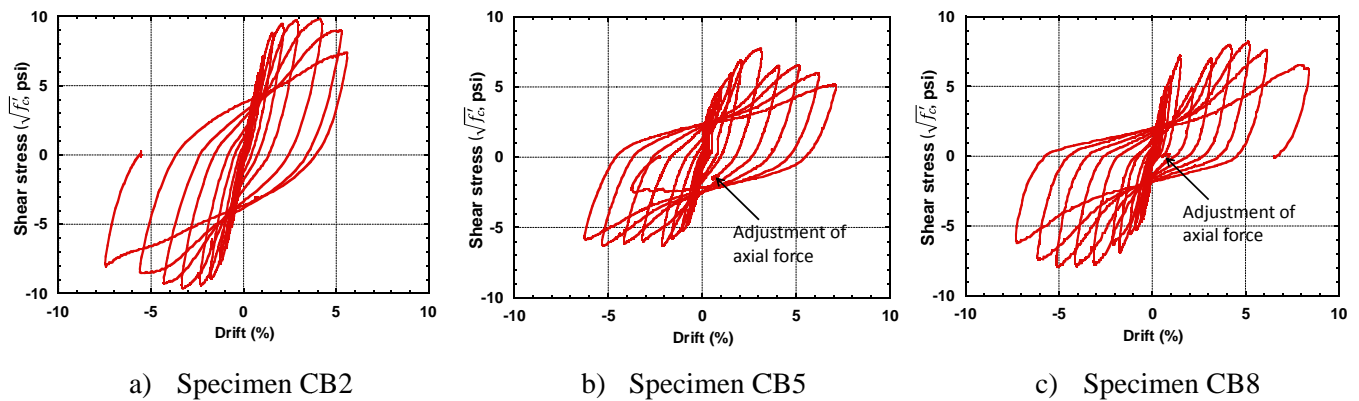
c) Specimen CB8

Fig. 6 – Shear stress versus drift hysteresis for Specimens CB2, CB5 and CB8

The average shear stress versus drift responses for Specimens CB2 and CB5 with $l_n/h = 3.0$, and Specimen CB8 with $l_n/h = 2.0$, are shown in Fig. 6. As can be seen in Fig. 6a, Specimen CB2, with HE 55/35 fibers at a 1.25% volume fraction, was subjected to a peak shear stress of nearly $10\sqrt{f'_c}$ [psi]. Peak drift in the positive

7

direction (nearly 6%) was limited by the test setup. In the negative loading direction, this specimen sustained a drift of approximately 7.5% and an average shear stress of $8\sqrt{f'_c}$ [psi]. Damage observed in Specimen CB2 at various drift levels is shown in Fig. 7.
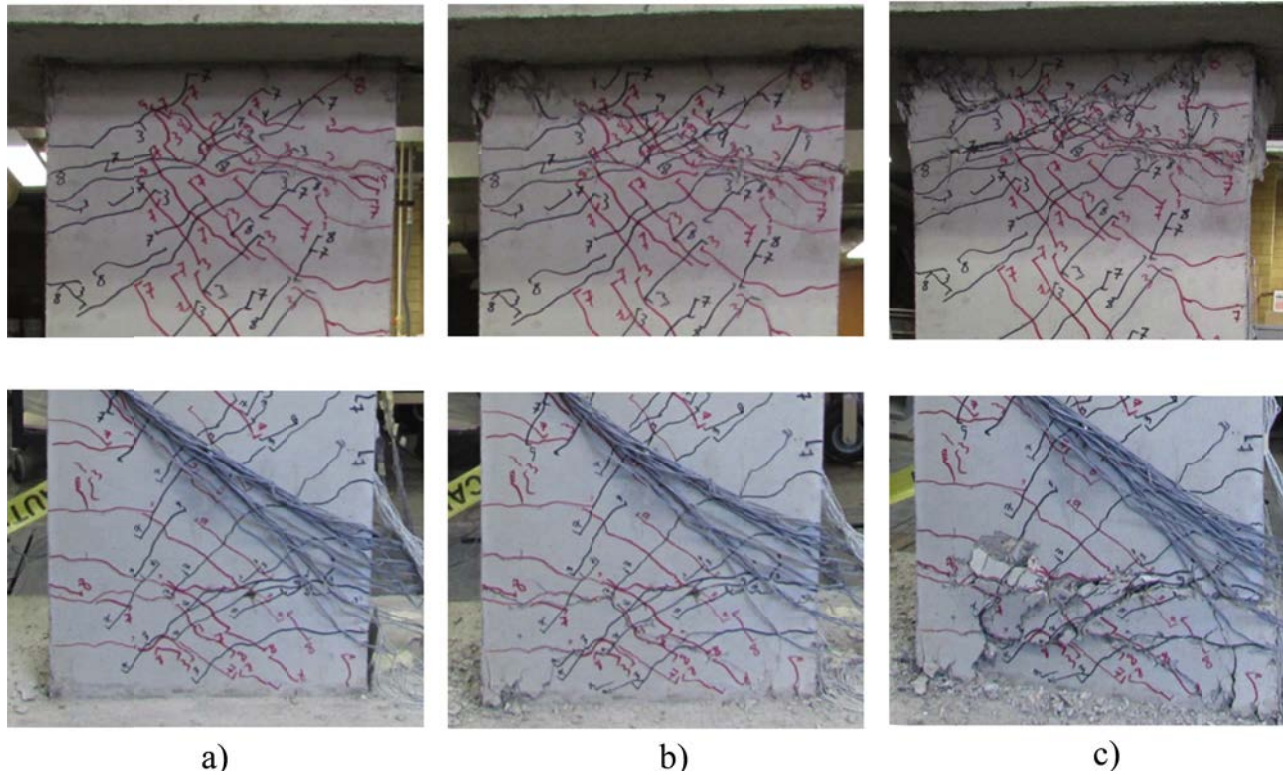
Fig. 7 - Damage at both ends of Specimen CB2 at approximately a) 2.0% drift, b) 4.0% drift, c) 5.5% drift

The response of Specimen CB5 (Fig. 6b), with RC 80/30 BP fibers at a 1.0% volume fraction, was similar to that of Specimen CB2 in terms of drift capacity. This specimen, however, was designed for a lower shear stress demand due to the use of an SFRC material with a 1.0% volume fraction. Peak shear stress in this specimen was close to $8\sqrt{f'_c}$ [psi] at 3.0% drift. Upon unloading after reaching 3.0% drift, the bolts connecting the vertical steel links used to keep the top block horizontal and provide restraint against axial expansion were loosened in order to control the axial force developed in the specimen and prevent further increases in applied shear during subsequent loading. This led to a reduction in flexural strength, which limited the applied shear during subsequent drift cycles to $6.6\sqrt{f'_c}$ [psi]. This test was terminated during the 7.0% drift cycle.

The average shear stress versus drift response for Specimen CB8, with $l_n/h = 2.0$ and a 1.5% volume fraction of RC 80/30 BP fibers, is shown in Fig. 6c. Compared to the behavior of Specimens CB2 and CB5, the hysteresis loops of Specimen CB8 were more "pinched", as expected, due to the lower l_n/h ratio. Peak shear stress for this specimen was approximately $8\sqrt{f'_c}$ [psi]. As was done for Specimen CB5, the axial force for Specimen CB8 was adjusted upon unloading from positive 1.75% drift, which caused the subsequent drop in strength. Specimen CB8 sustained a cycle at 6% drift with a peak shear stress of approximately $7.5\sqrt{f'_c}$ [psi]. This specimen was then pushed to a final cycle to 7.5% and 8.2% drift in the negative and positive loading direction, respectively, reaching a peak shear stress of approximately $6\sqrt{f'_c}$ [psi].

A summary of key response parameters for all coupling beam specimens, including peak shear stress demand, peak axial load, and average drifts (between positive and negative drifts) for the last cycle completed prior to exceeding a 20% and 30% strength loss in either direction, is presented in Table 1.

4. Estimation of flexural strength

Estimating the peak flexural strength of SFRC coupling beams with reasonable accuracy is critical, as strength under-predictions would lead to an underestimation of shear demand. Two critical sections for flexure must be considered, the wall-to-coupling beam interface and the section at the end of the dowel reinforcement.

The peak flexural strength for each of the test specimens at the wall-to-coupling beam interface was estimated using a plastic section analysis assuming that all reinforcement over the tension half of the beam depth was stressed at $1.1(f_y)_{measured}$ and that the main compression reinforcement was stressed at $(f_y)_{measured}$. For cases in which no information is available on actual yield strength, the use of $1.25f_y$ and f_y for the tension and compression steel is recommended, respectively. The compression zone was assumed to be stressed at $0.85f'_c$ over a depth a required for equilibrium of normal forces (including axial force). In the calculation of flexural strength, the peak axial force developed during the tests was used. For design purposes, however, it is recommended that strength calculations be ran without axial force and with an axial force of $0.1f'_cA_g$. Figure 8 shows the assumed stress distribution at the beam ends.

Excellent agreement was obtained between the calculated and experimental flexural strengths developed at the wall-to-coupling beam interface for all specimens that exhibited a flexurally-dominated response (Specimens CB2 through CB8). Except for Specimen CB4, calculated strength ranged between 92% and 100% of the peak experimental moment. Calculated strength of Specimen CB4 was 108% of the peak applied moment.

For the section at the end of the dowel reinforcement, incorporation of the post-cracking tensile strength of the SFRC led in some cases to significant overestimations of flexural strength, particularly for Specimens CB6 through CB8 with a fiber volume fraction of 1.5%. This is not unexpected, however, as the disturbance created by the termination of the dowel reinforcement, combined with the presence of two sets of hoops at the end of the dowels, weakened that section. Further, it is possible that the closely spaced hoop reinforcement at the coupling beam ends led to a tendency for fibers towards a vertical (perpendicular to longitudinal axis) orientation. The calculated flexural strength at the end of the dowel reinforcement, neglecting any contribution from the post-cracking strength of SFRC, also agreed well with the experimental strengths, with calculated strengths ranging between 0.97 and 1.12 of the maximum applied moment at that section.

For Specimens CB2 through CB8, the shear associated with the calculated flexural strength at the end of the dowels (without fibers) ranged between 102% and 110% of the shear corresponding to the calculated flexural strength at the beam end. This ratio led to satisfactory spread of plasticity at the end of the coupling beams.
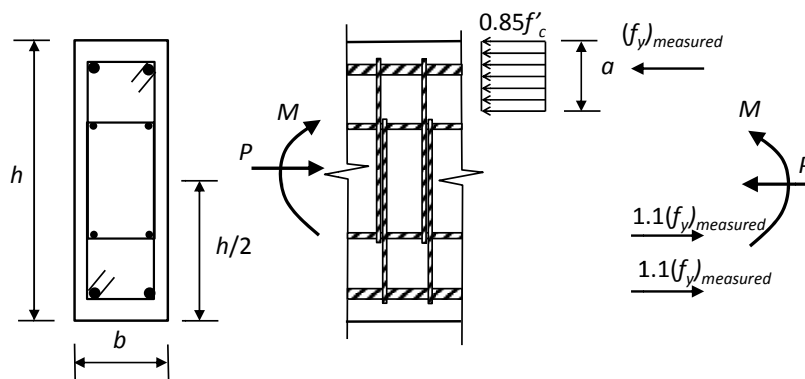
Fig. 8 - Assumed stress distribution for calculation of expected or probable moment strength in test specimens

5. SFRC material versus coupling beam performance

In order to establish a link between material behavior and coupling beam performance in terms of peak shear stress and drift capacity, the SFRCs investigated were lumped into three classes. Class 1 SFRC represents a material with a post-cracking tensile strength greater than the first cracking strength when subjected to direct tension. Thus, of all the SFRCs investigated, only that with a 1.5% volume fraction of RC 80/30 BP fibers would qualify as a Class 1 SFRC. Class 2 and Class 3 SFRCs, both tensile softening materials, are meant to represent

materials such as those used in Specimen CB2 (HE 55/35 fibers at V_f = 1.25%) and Specimen CB5 (RC 80/30 BP fibers at V_f = 1.0%), respectively. Performance criteria based on the results from four-point bending tests of un-notched beams are proposed to classify SFRCs as Class 1, Class 2 and Class 3 as follows:

- Class 1 SFRC:
  - o Peak post-cracking strength greater than or equal to 1.2 times the first cracking strength *and* greater than or equal to $12\sqrt{f_c}$ [psi]
  - o Residual strength at mid-span deflection of *L*/150, where *L* is the beam span length, greater than or equal to 0.4 times the peak post-cracking strength

- Class 2 SFRC:
  - o Peak post-cracking strength greater than or equal to the first cracking strength *and* greater than or equal to $9\sqrt{f_c}$ [psi]
  - o Residual strength at mid-span deflection of *L*/150 greater than or equal to 0.4 times the peak post-cracking strength

- Class 3 SFRC:
  - o Peak post-cracking strength greater than or equal to 0.8 times the first cracking strength *and* greater than or equal to $7.5\sqrt{f_c}$ [psi]
  - o Residual strength at mid-span deflection of *L*/150 greater than or equal to 0.4 times the peak post-cracking strength
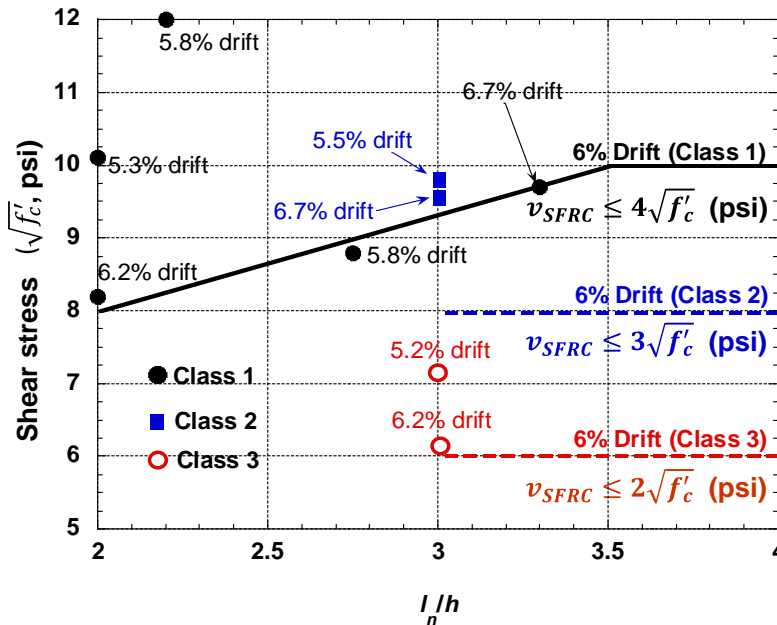
Fig. 9 - Recommended coupling beam shear stress-drift limits for Class 1, Class 2 and Class 3 SFRCs

Based on the performance of the test coupling beams, relationships between peak shear stress and span-to-depth ratio are proposed corresponding to an estimated 6% drift capacity for coupling beams constructed with each of the three classes of SFRC (Fig. 9). Class 1 SFRCs can be used for coupling beams with $l_n/h \geq 2.0$. Class 2 and Class 3 SFRCs, on the other hand, are only recommended for use in coupling beams with $l_n/h \geq 3.0$. Along with the peak shear stress limits, limits are also imposed on the calculated shear stress demand on the SFRC in the middle portion of the beam, v_{SFRC}. This shear stress demand is calculated as the difference between the expected shear stress and the nominal shear stress contributed by the transverse reinforcement, based on a 45-degree truss analogy and assuming yielding of the transverse steel.

Data points in Fig. 9 correspond to the test results for Specimens CB2 through CB5, and Specimens CB7 and CB8, as well as test specimens with a span-to-depth ratio of 2.2, 2.75 and 3.3 reported in Parra-Montesinos et al. (2014), which were constructed with a material that qualifies as Class 1 SFRC. Data for Specimen CB1 were excluded as the shear stress demand on the SFRC for this specimen exceeded the recommended limit of $4\sqrt{f'_c}$ [psi]. On the other hand, Specimen CB6 was excluded because that specimen had a $l_n/h = 2.0$ and the material used did not qualify as a Class 1 SFRC.

It should be noted that some test specimens exhibited a drift capacity less than 6.0%. In all cases but one, however, the peak shear stress in those specimens was greater than the recommended shear stress limit. An attempt was thus made to estimate the drift capacity based on the recommended shear stress limit. The exception to this was the specimen with $l_n/h = 2.75$ reported in Parra-Montesinos et al. (2014), which exhibited a drift capacity of 5.8%. Given the additional data corresponding to coupling beams with $l_n/h < 2.75$ and $l_n/h = 3.0$, and the closeness of this shear stress to the proposed limit, the recommended limit is believed to be acceptable.

6. Conclusions

An experimental study consisting of the testing of eight large-scale coupling beams under displacement reversals was conducted to evaluate the use of various types of steel fiber reinforced concrete (SFRC) in order to eliminate the need for diagonal bars and relax transverse reinforcement requirements in earthquake-resistant coupling beams. Experimental variables were span-to-depth ratio, type of SFRC (fiber type and dosage), and peak shear stress demand. The following conclusions are based on the observations and results obtained from the coupling beam tests as well as the SFRC material tests.

- In general, SFRC coupling beams with $l_n/h \geq 2.0$ and no diagonal reinforcement can achieve drift capacities of at least 5% and exhibit stable, flexurally-dominated behavior while undergoing shear stress reversals ranging from 6 to $10\sqrt{f'_c}$ [psi].
- The use of RC 80/30 BP fibers at a 1.5% volume fraction resulted in a post-cracking strength greater than the first cracking strength under direct tension and pronounced deflection hardening under four-point bending. A material with such behavior (classified as Class 1 SFRC) is needed in order to achieve 6% drift capacity in coupling beams with span-to-depth ratios between 2.0 and 3.0 and shear stresses of up to 8 and $10\sqrt{f'_c}$ [psi], respectively.
- Coupling beams with $l_n/h \geq 3.0$, no diagonal bars, and constructed with materials satisfying the proposed requirements for Class 2 and Class 3 SFRCs, may achieve a drift capacity of 6% depending on the shear stress demand. A 6% drift capacity can be achieved when shear stresses are limited to $8\sqrt{f'_c}$ [psi] for Class 2 SFRC and to $6\sqrt{f'_c}$ [psi] for Class 3 SFRC. Until further experimental data become available, these materials are not recommended for use in coupling beams without diagonal reinforcement and $l_n/h < 3.0$.
- Transverse reinforcement requirements for potential plastic hinge regions in columns of special moment frames in ACI 318-14 are adequate for confinement of the end regions of coupling beams, over a length of half the beam depth from the wall faces. Transverse reinforcement in the middle region of SFRC coupling beams, on the other hand, must be designed such that the expected shear stresses to be resisted by the SFRC material do not exceed 4, 3 and $2\sqrt{f'_c}$ [psi] for Class 1, Class 2 and Class 3 SFRC, respectively.
- Two critical sections must be considered for calculation of flexural strength, the wall-to-coupling beam interface and the section at the termination of the dowel reinforcement. Expected or probable flexural capacity can be estimated based on the use of a plastic stress distribution assuming all reinforcement over the tension half of the beam depth reaches a stress of 1.1 times the measured yield strength or 1.25 times the nominal yield strength. It is recommended that the contribution of the fiber reinforcement to flexural strength at the termination of the dowels be ignored. It is also recommended that strength calculations be ran without axial force and with an axial force of $0.1f'_cA_g$.

- For adequate spread of plasticity, intermediate dowel reinforcement at the beam ends must be designed such that the shear associated with the expected flexural strength at the end of the dowels ranges between approximately 1.0 and 1.1 times the shear corresponding to the expected flexural strength at the beam ends.

7. Acknowledgements

8. References

[1] ACI Committee 318 (2014): *Building code requirements for structural concrete (ACI318-14)*. American Concrete Institute, Farmington Hills, MI, USA.

[2] Canbolat A, Parra-Montesinos G, Wight JK (2005): Experimental study on seismic behavior of high-performance fiber-reinforced cement composite coupling beams. *ACI Structural Journal*, **102** (1), 159-166.

[3] Kopczynski C, Whiteley M (2016): Lincoln square expansion. Steel fiber reinforced concrete solves seismic design challenge. *Structure Magazine*, March 2016, 42-44.

[4] Lequesne R (2011): Behavior and design of high-performance fiber-reinforced concrete coupling beams and coupled-wall systems. *Ph.D. dissertation*, The University of Michigan, Ann Arbor, MI, USA.

[5] Lequesne R, Parra-Montesinos GJ, Wight JK (2013): Seismic behavior and detailing of high-performance fiber-reinforced concrete coupling beams and coupled wall systems. *Journal of Structural Engineering*, ASCE, **139** (8), 1362-1370.

[6] Paulay T (1971): Coupling beams of reinforced concrete shear walls. *Journal of the Structural Division*, Proceedings ASCE, **97** (ST3), 843-861.

[7] Paulay T, Binney JR (1974): Diagonally reinforced coupling beams of shear walls. *ACI Publication SP-42*, 579- 598

[8] Paulay T, Santhakumar AR (1976): Ductile behavior of coupled shear walls. *Journal of the Structural Division*, Proceedings ASCE, **102** (ST1), 99-108.

[9] Parra-Montesinos GJ, Wight JK, Kopczynski C, Lequesne R, Setkit M, Conforti A, Ferzli J (2014): High-performance fiber reinforced concrete coupling beams: from research to practice. *Tenth U.S. National Conference on Earthquake Engineering*, Anchorage, AK, USA.

[10]Setkit M (2012): Seismic behavior of slender coupling beams constructed with high-performance fiber-reinforced concrete. *Ph.D. dissertation*, The University of Michigan, Ann Arbor, MI, USA.

9. Unit conversions

1 in. = 25.4 mm

1 ksi = 1000 psi = 6.89 MPa

$\sqrt{f'_c}$ [psi] $= \frac{1}{12}\sqrt{f'_c}$ [MPa]

Reinforcing bar diameters: #3 =10 mm; #4 = 13 mm; #5 = 16 mm; #6 = 19 mm